CURRENT ONCOLOGY
A Canadian Cancer Research Journal

ORIGINAL ARTICLE

A new predictive scoring system based on clinical data and computed tomography features for diagnosing *EGFR*-mutated lung adenocarcinoma

Y. Cao MD* and H. Xu MD*

ABSTRACT

Background We aimed to develop a new *EGFR* mutation–predictive scoring system to use in screening for *EGFR*-mutated lung adenocarcinomas (LACs).

Methods The study enrolled 279 patients with LAC, including 121 patients with *EGFR* wild-type tumours and 158 with *EGFR*-mutated tumours. The Student t-test, chi-square test, or Fisher exact test was applied to discriminate clinical and computed tomography (CT) features between the two groups. Using a principal component analysis (PCA) model, we derived predictive coefficients for the presence of *EGFR* mutation in LAC.

Results The *EGFR* mutation–predictive score includes sex, smoking history, homogeneity, ground-glass opacity (GGO) on imaging, and the presence of pericardial effusion. The PCA predictive model took this form:

sex × 16 + smoking history × 15 + GGO × 12 + pericardial effusion × 10 + emphysema × 11.

Model scores ranged from 79 to 147. The area under the receiver operating characteristic curve was 0.752 [95% confidence interval (CI): 0.697 to 0.801] in the LAC population at the optimal cut-off value of 109, and the sensitivity and specificity were 68.4% (95% CI: 60.5% to 75.5%) and 74.4% (95% CI: 65.6% to 81.9%) respectively.

Conclusions The *EGFR* mutation risk scoring system based on clinical data and CT features is noninvasive and user-friendly. The model appears to frame a positive predictive value and was able to determine the value of repeating a biopsy if tissue is limited.

Key Words Computed tomography, epidermal growth factor receptor, lung cancer, adenocarcinoma

Curr Oncol. 2018 April;25(2):e132-e138 www.current-oncology.com

INTRODUCTION

The cancer-related lethality rate for lung and bronchus cancer is high worldwide, accounting annually for approximately 0.16 million deaths in the United States[1] and 0.61 million deaths in China[2]. Because of different treatment methods, lung cancers are classified into two major categories: non-small-cell lung cancer (NSCLC) and small-cell lung cancer. Lung adenocarcinomas (LACs) represent a major proportion of the NSCLC group[3].

Earlier studies have demonstrated that pathology classification has no significant effect on treatment and prognosis in most subtypes of NSCLC (neuroendocrine tumours excepted)[4,5]. However, advances in research and continuous improvements in gene test technology have revealed that not all NSCLCs respond to treatment in a consistent manner. Increasing attention has been paid to the individual treatment of some particular lung cancer subtypes, among which the most studied is targeted therapy for lung cancer with gene mutations[6]. Therapy with an

Correspondence to: Yiyuan Cao or Haibo Xu, Department of Radiology, Zhongnan Hospital of Wuhan University, Wuhan University, 169 Donghu Road, Wuhan, Hubei 430071 P.R.C.
E-mail: caoyy@whu.edu.cn or haiboxu1120@hotmai.com ■ **DOI:** https://doi.org/10.3747/co.25.3805

epidermal growth factor receptor (EGFR) tyrosine kinase inhibitor, which is aimed explicitly at *EGFR* mutations in lung cancer, delays progression in patients with *EGFR* mutations[7,8]. Compared with conventional chemotherapy, therapy with an EGFR tyrosine kinase inhibitor is associated with fewer complications and reduced toxicity[8,9]. Nevertheless, therapy with a tyrosine kinase inhibitor is not effective in the treatment of wild-type NSCLC[10].

EGFR mutations are among the most common genetic mutations in lung cancer, and they represent the most frequent mutation in LAC[11]. For genotyping the tumour, histologic samples of plasma or another body fluid must be obtained[12–14]. In some cases, obtaining those materials is challenging[15], and testing has always been problematic. Identification of the *EGFR* mutation status in NSCLC without a molecular examination would be beneficial for choosing treatment.

Some studies have attempted to determine the relationship between molecular findings and certain disease features such as sex, smoking status, the presence of ground-glass opacity (GGO) on imaging, and other features[16–18]. However, most of the reports described only the features with statistical significance, whose clinical value is limited. We retrospectively analyzed a cohort of East Asian patients with LAC who had been tested for *EGFR* mutations in our hospital. We hoped to develop a scoring system for *EGFR* mutation screening in LAC, thus providing supplementary diagnostic information for new patients from whom tissue specimens cannot be obtained.

METHODS

Patient Selection

This retrospective study was approved by the institutional review board. Informed consent was waived. Results of consecutive *EGFR* mutation tests in lung cancer were obtained from the hospital's pathology database.

Between January 2014 and October 2016, 365 patients underwent *EGFR* mutation testing. Patients were excluded if they had no computed tomography (CT) imaging data within 1 month before surgery; if they had no non-contrast CT data or contrast-enhanced CT data available; if pathology had confirmed that the lesion was not LAC; if multiple tumours were present in the lung, such that the relationship between the tumour and the pathology results could not be independently determined; if tumour boundaries could not be distinguished; and if other types of mutations or the *EGFR* T790M mutation was present. As a result, 86 patients were excluded.

For the remaining 279 patients, clinical and pathology data were collected. Clinical data included age, sex, tumour staging, and smoking status (the definition of a "nonsmoker" was never having smoked). Tumour staging reflected the 7th edition of the American Joint Committee on Cancer staging manual[19].

Histologic Evaluation and Molecular Analysis

Per routine procedure at our hospital, after histology specimens were obtained, they were formalin-fixed and then stained with hematoxylin–eosin. Immunohistochemical analysis was used to assess tumours that could not be diagnosed by routine procedures. Two pathologists reviewed the pathology specimens and recorded the results separately. For all disagreements about diagnosis, the two pathologists discussed the findings to obtain a final consensus. Diagnostic criteria were based on the 2015 World Health Organization classification of lung tumours[20].

A fluorescence polymerase chain reaction diagnostic kit (Amoy Diagnostics, Xiamen, P.R.C.) was used to perform an *EGFR* gene mutation analysis for exons 18–21 in the specimens. The test result was determined by the cycle threshold score. The result was considered to be strongly positive at a cycle threshold score between 0 and 26. A cycle threshold score between 26 and 29 indicated weak positive expression. If the score was greater than 29, the result was considered negative.

CT Imaging

Two CT systems (Sensation 16 and Somatom Definition: Siemens Medical Systems, Erlangen, Germany) were involved in the retrospective study. Images were obtained at 5 mm section thickness, without a gap, using the mediastinal algorithm in both CT systems as a "mediastinal window," and at 1 mm section thickness, without a gap, using the high-frequency algorithm as a "lung window." The main imaging parameters were 120 kV and 100 mA (Sensation 16) and 120 kV and 100–400 mA with dose modulation (Somatom Definition).

We selected Ultravist (Ultravist 300: Bayer Pharma, Berlin, Germany) as the contrast medium. Contrast-enhanced images were collected with a 45 s delay after intravenous injection of the contrast medium. The injection rate was 3.0 mL/s, and the dose was based on the patient's weight.

CT Interpretation

All images were reviewed by two independent board-certified thoracic radiologists. Both radiologists were unaware of the pathology diagnosis and the *EGFR* test results. All features were evaluated on cross-sectional images, including the lung window and the mediastinal window. Discrepancies between the radiologists were resolved by discussion. The final measurements and counts were obtained by averaging the results from the two radiologists.

In addition to morphologic features, we recorded the tumour disappearance rate (TDR), relative enhancement, lobulation, pleural retraction, calcification, bubble-like lucency, air bronchography, pneumonia-like consolidation, GGO, vessel convergence sign, spiculation, pericardial effusion, pleural effusion, and mediastinal lymph node metastasis.

These definitions of the imaging features were used:

- $\text{TDR} = 1 - \text{MaxD}_{\text{mediastinal}} \times \text{MinD}_{\text{mediastinal}} / (\text{MaxD}_{\text{lung}} \times \text{MinD}_{\text{lung}})$, where $\text{MaxD}_{\text{mediastinal}}$ and $\text{MinD}_{\text{mediastinal}}$ represent the measurements of the longest and shortest diameters of the tumour in millimeters in the mediastinal window; and $\text{MaxD}_{\text{lung}}$ and $\text{MinD}_{\text{lung}}$ represent the measurements of the longest and shortest diameters of the tumour in millimeters in the lung window[21]. The cut-off value for TDR was 0.5.

- Relative enhancement = $(A_{post} - A_{pre}) / E_{art}$, where A_{post} represents the attenuation of the tumour in the contrast-enhanced image; A_{pre} represents the attenuation of the tumour in the non-contrast image; and E_{art} indicates the attenuation of the descending aorta in the contrast-enhanced image[18].

- Lobulation = portion of the tumour surface exhibiting a slightly wavy appearance, with the exception of regions abutting the pleura, where "lobulation" was calculated based on numbers so as to divide the patients into two groups.

- Pneumonia-like consolidation = a homogenous or heterogeneous opacity lesion in the lung
  Unlike GGO, pneumonia-like consolidation effaces the blood vessel shadows, and occasionally an air bronchogram can be displayed without any bacterial or obstructive pneumonia[16].

- Spiculation = cut-off of the burr diameter, where the cut-off was defined so as to divide the patients into two groups. That cut-off was 2 mm.

Statistical Analysis

Most of the statistical analyses were performed using the SPSS software application (version 21.0: IBM, Armonk, NY, U.S.A.). The receiver operating characteristic curve was analysed using the MedCalc software application (version 15.8: MedCalc Software, Ostend, Belgium). Categorical variables were analyzed using the chi-square or Fisher exact test, as appropriate. Continuous variables were analyzed using the Student t-test. A p value less than 0.05 was considered statistically significant. Collinearity diagnosis was applied to detect collinearity between the features. If no collinearity was noted between the parameters, the parameters were loaded in series into a multivariable logistic regression model. Otherwise, PCA was used to solve the problem. The new *EGFR* mutation predictive score was derived by multiplying the regression of the PCA coefficient for the significant features by 10 and then rounding to the nearest integer. All significant features were thereafter calculated together in both groups, using the resulting numbers as scores. The final data were used to generate the receiver operating characteristic curve and to calculate the area under the curve. The Youden index was used to calculate the optimal cut-off.

RESULTS

The differences between the two radiologists were, for the presence of calcification, 1 in 279 patient exams (0.36%); for the presence of air bronchogram, 3 in 279 patient exams (1.08%); for vessel convergence sign, 6 in 279 patient exams (2.15%); and for pneumonia-like consolidation, 5 in 279 patient exams (1.79%).

Patient Characteristics

Of the 279 patients with LAC involved in the analysis, 158 harboured an *EGFR* mutation: exon 18 mutation in 7 patients (4.43%), exon 19 mutation in 67 patients (42.41%), exon 20 mutation in 7 patients (4.43%), and exon 21 mutation in 73 patients (46.20%). The remaining 4 patients each had 2 mutations: an exon 21 mutation and an exon 19 mutation in 2 patients, and an exon 21 mutation and an exon 20 mutation in 2 patients. Of the 279 patients overall, 150 underwent lung resection or open lung biopsy, 125 underwent CT-guided biopsy, and 4 underwent fibre-optic bronchoscopy–guided biopsy. *EGFR* mutations were more common in women ($n = 90$, $p < 0.001$), nonsmokers ($n = 120$, $p < 0.001$), and patients with less-severe emphysema ($n = 155$, $p = 0.002$). However, no significant differences in age or tumour staging were noted between the wild-type group and the *EGFR* mutation group (Table I).

CT Imaging Evaluation

In the *EGFR* mutation group, most of the tumours appeared homogenous in the contrast-enhanced image ($p < 0.001$). Ground-glass opacity appeared more common in patients with *EGFR*-mutated tumours (30 of 158) than in those with wild-type tumours (12 of 121, $p = 0.036$). Pericardial effusion was more frequently observed in patients with *EGFR*-mutated tumours (10 of 158, $p = 0.026$). No significant differences in location, attenuation, TDR, relative enhancement, pneumonia-type, lobulation, boundary, shape, spiculation, calcification, air bronchogram, cavitation, vascular convergence sign, pleural indentation, pleural effusion, and mediastinal lymph node metastasis were noted between the groups (Table II).

Collinear diagnosis revealed collinearity between emphysema and smoking history. We therefore used PCA to obtain the coefficients for each feature. Using the previous statistical results, we divided the parameters of each feature into two categories. We set the parameters that tended to diagnose *EGFR* mutation to 2; the remaining parameters were set to 1 (Table III). The original PCA predictive scoring model took this form:

$$\text{sex} \times 1.5986 + \text{smoking history} \times 1.4552 + \text{GGO} \times 1.1505 + \text{pericardial effusion} \times 1.0394 + \text{emphysema} \times 1.0609.$$

To facilitate clinical application, we multiplied the PCA coefficients of the significant feature by 10 and rounded to the nearest integer (Table III). The PCA predictive model thus took this form:

$$\text{sex} \times 16 + \text{smoking history} \times 15 + \text{GGO} \times 12 + \text{pericardial effusion} \times 10 + \text{emphysema} \times 11.$$

The receiver operating characteristic curve (Figure 1) used the final score as a variable (range: 79–148) and the genetic diagnosis as the dependent variable (1 = *EGFR*-mutated, 0 = wild-type). The area under the curve was 0.752 (95% CI: 0.697 to 0.801). The maximum value of the Youden index was 0.427, which corresponded to an optimal cut-off value of 109. When the calculated score was greater than 109, we tended to diagnose *EGFR* mutation. The sensitivity and specificity were 68.4% (95% CI: 60.5% to 75.5%) and 74.4% (95% CI: 65.6% to 81.9%) respectively.

TABLE I Clinical features of the patients

Feature	*EGFR* group			*p* Value[a]
	Overall	Wild-type	Mutated	
Age (years)				0.601
Median	60.84	61.29	60.49	
Range	32–85	32–82	41–85	
Sex				**<0.001**
Men	167	99	68	
Women	112	22	90	
Smoking history				**<0.001**
Smoker	127	89	38	
Nonsmoker	152	32	120	
Stage				0.276
IA	43	17	26	
IB	38	11	27	
IIA	9	5	4	
IIB	16	10	6	
IIIA	52	23	29	
IIIB	14	8	6	
IV	107	47	60	
Emphysema score				**0.002**
<8 (normal)	262	107	155	
≥8	17	14	3	

[a] Values in boldface type are statistically significant.

TABLE II Computed tomography imaging evaluation

Feature	*EGFR* group		*p* Value[a]
	Wild-type	Mutated	
Homogeneity after contrast			**0.002**
Heterogeneous	73	66	
Homogenous	48	92	
Tumour disappearance rate			0.054
<0.5	114	138	
≥0.5	7	20	
Ground-glass opacity			**0.036**
Present	12	30	
Absent	109	128	
Pericardial effusion			**0.026**
Present	1	10	
Absent	120	148	
Location			0.109
Inferior lobe of left lung	15	30	
Superior lobe of left lung	32	37	
Middle lobe of right lung	3	13	
Inferior lobe of right lung	33	38	
Superior lobe of right lung	38	40	
Mean pre-contrast attenuation	34.41 ±9.36	33.51 ±9.78	0.408
Mean relative enhancement	0.1853 ±0.0867	0.1863 ±0.0851	0.730
Pneumonia-type			0.411
Yes	9	8	
No	112	150	
Shape			0.793
Round or oval	83	102	
Irregular	45	59	
Lobulation			0.500
<6	86	118	
≥6	35	40	
Spiculation			0.516
Thin	49	62	
Thick	26	43	
Absent	46	53	
Boundary			0.191
Clear	54	83	
Obscure	67	75	
Calcification			0.186
Present	11	8	
Absent	110	150	
Cavitation			0.705
Present	22	26	
Absent	99	132	

DISCUSSION

Molecular analysis has always been the best choice for diagnosing *EGFR* mutation status. However, its application has been limited for various reasons. Some patients might not be able to undergo biopsy or surgery. Some medical centres might not have access to molecular profiling technology to perform the test. In addition, for some histology specimens, sufficient material might not be present to perform the test. We sought to develop an alternative method that is useful in patients who are unable to undergo molecular studies.

Our study was carried out in two parts. In the first part, we evaluated the relationship between the clinical and CT features associated with *EGFR* mutation. In LAC, *EGFR* mutation was associated with 6 features. In the second part, we used PCA to establish a predictive scoring model for *EGFR* mutation.

Our study focused on an East Asian population. Compared with patients of other ethnicities, East Asian patients with NSCLC have the highest rates of *EGFR* mutation[22,23]. We demonstrated that the *EGFR* mutation rate was statistically higher in women and nonsmokers. The *EGFR* mutation rate in our group was 56.63%, and female patients accounted for 56.96% of the population, which was consistent with findings in other studies[18,24]. Smoking history is also a frequently studied epidemiologic feature. Our result was similar to that in earlier studies[25,26].

TABLE II Continued

Feature	EGFR group		*p* Value[a]
	Wild-type	Mutated	
Air bronchogram			0.541
Present	21	32	
Absent	100	126	
Vascular convergence sign			0.087
Present	32	57	
Absent	89	101	
Pleural indentation			0.869
Present	64	82	
Absent	57	76	
Pleural effusion			0.444
Present	23	36	
Absent	98	122	
Mediastinal lymph node metastasis			0.063
Present	71	75	
Absent	50	83	

[a] Values in boldface type are statistically significant.

TABLE III The *EGFR*-mutation predictive score model, based on principal components analysis coefficient

Component	Coefficient	Score	Total score
Sex			
Woman	16	2	32
Man	16	1	16
Smoking status			
Nonsmoker	15	2	30
Smoker	15	1	15
Emphysema			
Less severe	10	2	20
Severe	10	1	10
Pericardial effusion			
Present	10	2	20
Absent	10	1	10
Homogeneity after contrast			
Homogenous	15	2	30
Heterogeneous	15	1	15
Ground-glass opacity			
Present	12	2	24
Absent	12	1	12

In addition to the foregoing demographic and epidemiologic features, our study also identified emphysema status as an important predictor. Results of the Goddard scoring system[27] revealed that the *EGFR* mutation rate was greater for patients having the mild type of emphysema (59.16%) than for those having the severe type (17.65%). We observed

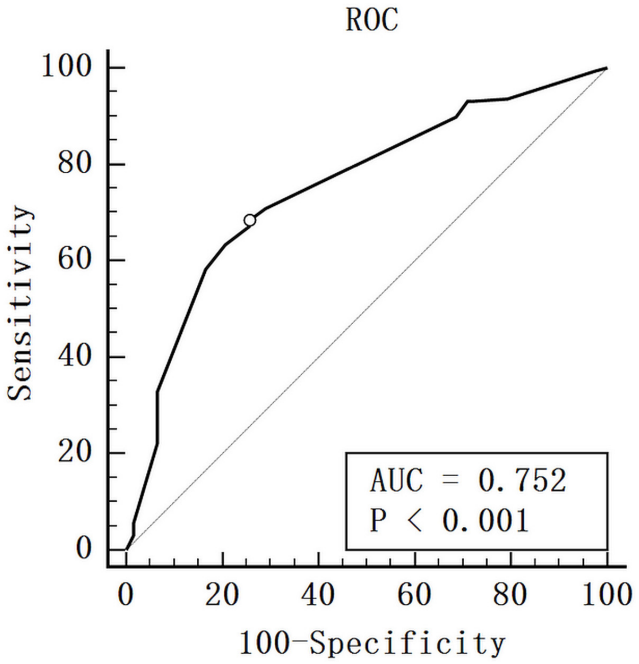

FIGURE 1 Receiver operating characteristic (ROC) of the *EGFR* mutation predictive score. AUC = area under the curve.

a correlation between smoking history and emphysema. The Goddard scoring system has certain advantages in clinical practice. The system requires only the CT image to be scored. If smoking history is not available, the Goddard score can provide some useful information.

We demonstrated that homogeneity and the presence of GGO and pericardial effusion differed statistically depending on mutation status. In the present study, wild-type tumours were more heterogeneous after contrast than were *EGFR*-mutated tumours. Research about this feature is limited[28]. Homogeneity before contrast was also studied, and no significant difference was noted by mutation status. It is possible that, compared with *EGFR*-mutated tumours, wild-type tumours cause more necrosis, making them appear more heterogeneous.

In the study of *EGFR* mutations in LAC, GGO is one of the most common imaging features[17,18,24]. It appears more frequently in *EGFR*-mutated LAC, and that finding has not caused much controversy. In the present study, pericardial effusion was observed more frequently in patients with *EGFR* mutation, and that condition is always caused by pericardial metastasis. Prior studies have demonstrated that, compared with *EGFR*-mutated LAC tumours, those with the *ALK* rearrangement are more often associated with pleural or pericardial metastases[29]. Research focused on the relationship between pericardial metastasis and *EGFR* mutation is limited, and future studies should focus more on this feature.

In addition to a lack of statistically significant features, most of our results are consistent with prior research, with the exception of pneumonic-type lesions. Pneumonic-type lesions were previously known as consolidation-type lung cancer and were typically misdiagnosed as inflammatory

pulmonary consolidation. A few studies demonstrated that patients with pneumonic-type lesions experience a significantly increased incidence of *EGFR* mutations, independent of sex, histologic type, and smoking history[16]. That research focused on patients before surgery, and our study focused on biopsy patients. In addition, biopsy specimens are considered highly sensitive for *EGFR* detection[30,31]. However, differences in patient selection might explain the different results.

In the first part of the study, we identified numerous significant features, but still found it difficult to reach a final diagnosis. Our challenge was how to integrate the parameters. In the second part of the study, we used clinical data and CT imaging to establish a practical predictive scoring system that could identify *EGFR* mutation. This *EGFR* mutation predictive scoring system comprises 6 features, including sex, smoking status, homogeneity, emphysema status, pericardial effusion status, and GGO on imaging. Those features were selected from among 24 clinical factors and CT features of LAC. The scoring system can differentiate wild-type or *EGFR*-mutated tumours with moderate accuracy based on the resulting score. The system uses PCA coefficients to convert the features of LAC into qualitative data. The area under the curve was 0.752 in the LAC population, and the sensitivity and specificity were 68.4% (95% CI: 60.5% to 75.5%) and 74.4% (95% CI: 65.6% to 81.9%) respectively.

Our scoring system is easily applied and does not require extensive clinical testing. It can provide complementary information for patients who cannot undergo genetic testing or for patients treated at clinical centres with limited access to molecular profiling. When false-negative molecular results are suspected, the scoring system can be used to assist in the diagnosis and to determine whether a repeat biopsy is necessary.

Our study has some limitations. First, the number of patients was not large, which could affect the accuracy of the prediction model. Second, because of geographic constraints, we focused on an East Asian population, and the results might therefore not have significant implications for other ethnic groups. Third, the scanning parameters were not exactly same in the two CT systems, which might have contributed bias.

CONCLUSIONS

Although considerable research has focused on *EGFR* mutation in LAC, the present study is the first to use a scoring system to predict *EGFR* mutation status in an East Asian population. Earlier research studied Caucasian populations[32]. Prospective studies will have to determine whether the *EGFR* mutation scoring system can be used to inform treatment decisions or to predict tumour genotype.

CONFLICT OF INTEREST DISCLOSURES

We have read and understood *Current Oncology*'s policy on disclosing conflicts of interest, and we declare that we have none.

AUTHOR AFFILIATIONS

*Department of Radiology, Zhongnan Hospital of Wuhan University, Wuhan, Hubei, P.R.C.

REFERENCES

1. Siegel RL, Miller KD, Jemal A. Cancer statistics, 2016. *CA Cancer J Clin* 2016;66:7–30.
2. Chen W, Zheng R, Baade PD, *et al.* Cancer statistics in China, 2015. *CA Cancer J Clin* 2016;66:115–32.
3. de Lima Lopes G, Segel JE, Tan DS, Do YK, Mok T, Finkelstein EA. Cost-effectiveness of epidermal growth factor receptor mutation testing and first-line treatment with gefitinib for patients with advanced adenocarcinoma of the lung. *Cancer* 2012;118:1032–9.
4. Sakashita S, Sakashita M, Sound Tsao M. Genes and pathology of non–small cell lung carcinoma. *Semin Oncol* 2014;41:28–39.
5. Alexander M, Wolfe R, Ball D, *et al.* Lung cancer prognostic index: a risk score to predict overall survival after the diagnosis of non-small-cell lung cancer. *Br J Cancer* 2017;117:744–51.
6. Buettner R, Wolf J, Thomas RK. Lessons learned from lung cancer genomics: the emerging concept of individualized diagnostics and treatment. *J Clin Oncol* 2013;31:1858–65.
7. Lee CK, Brown C, Gralla RJ, *et al.* Impact of EGFR inhibitor in non–small cell lung cancer on progression-free and overall survival: a meta-analysis. *J Natl Cancer Inst* 2013;105:595–605.
8. Hoffknecht P, Tufman A, Wehler T, *et al.* Efficacy of the irreversible ErbB family blocker afatinib in epidermal growth factor receptor (EGFR) tyrosine kinase inhibitor (TKI)–pretreated non-small-cell lung cancer patients with brain metastases or leptomeningeal disease. *J Thorac Oncol* 2015;10:156–63.
9. Ozkan E, West A, Dedelow JA, *et al.* CT gray-level texture analysis as a quantitative imaging biomarker of epidermal growth factor receptor mutation status in adenocarcinoma of the lung. *AJR Am J Roentgenol* 2015;205:1016–25.
10. Lee JK, Hahn S, Kim DW, *et al.* Epidermal growth factor receptor tyrosine kinase inhibitors vs conventional chemotherapy in non–small cell lung cancer harboring wild-type epidermal growth factor receptor: a meta-analysis. *JAMA* 2014;311:1430–7.
11. Antonicelli A, Cafarotti S, Indini A, *et al.* EGFR-targeted therapy for non–small cell lung cancer: focus on *EGFR* oncogenic mutation. *Int J Med Sci* 2013;10:320–30.
12. Wakelee HA, Gadgeel SM, Goldman JW, *et al.* Epidermal growth factor receptor (*EGFR*) genotyping of matched urine, plasma and tumor tissue from non–small cell lung cancer (NSCLC) patients (pts) treated with rociletinib [abstract 9001]. *J Clin Oncol* 2016;34:. [Available online at: https://meetinglibrary.asco.org/record/123411/abstract; cited 30 December 2017]
13. Reckamp KL, Melnikova VO, Karlovich C, *et al.* A highly sensitive and quantitative test platform for detection of NSCLC *EGFR* mutations in urine and plasma. *J Thorac Oncol* 2016;11:1690–700.
14. Weber B, Meldgaard P, Hager H, *et al.* Detection of *EGFR* mutations in plasma and biopsies from non–small cell lung cancer patients by allele-specific PCR assays. *BMC Cancer* 2014;14:294.
15. Kim H, Chae KJ, Yoon SH, *et al.* Repeat biopsy of patients with acquired resistance to EGFR TKIs: implications of biopsy-related factors on T790M mutation detection. *Eur Radiol* 2018;28:861–8.
16. Liu J, Shen J, Yang C, *et al.* High incidence of *EGFR* mutations in pneumonic-type non–small cell lung cancer. *Medicine (Baltimore)* 2015;94:e540.
17. Hsu JS, Huang MS, Chen CY, *et al.* Correlation between *EGFR* mutation status and computed tomography features in patients with advanced pulmonary adenocarcinoma. *J Thorac Imaging* 2014;29:357–63.
18. Liu Y, Kim J, Qu F, *et al.* CT features associated with epidermal growth factor receptor mutation status in patients with lung adenocarcinoma. *Radiology* 2016;280:271–80.

19. Edge SB, Compton CC. The American Joint Committee on Cancer: the 7th edition of the AJCC cancer staging manual and the future of TNM. *Ann Surg Oncol* 2010;17:1471–4.
20. Travis WD, Brambilla E, Nicholson AG, *et al.* The 2015 World Health Organization classification of lung tumors: impact of genetic, clinical and radiologic advances since the 2004 classification. *J Thorac Oncol* 2015;10:1243–60.
21. Nakada T, Okumura S, Kuroda H, *et al.* Imaging characteristics in *ALK* fusion–positive lung adenocarcinomas by using HRCT. *Ann Thorac Cardiovasc Surg* 2015;21:102–8.
22. Dearden S, Stevens J, Wu YL, Blowers D. Mutation incidence and coincidence in non small-cell lung cancer: meta-analyses by ethnicity and histology (mutMap). *Ann Oncol* 2013;24:2371–6.
23. El-Telbany A, Ma PC. Cancer genes in lung cancer: racial disparities: are there any? *Genes Cancer* 2012;3:467–80.
24. Ha SY, Choi SJ, Cho JH, *et al.* Lung cancer in never-smoker Asian females is driven by oncogenic mutations, most often involving *EGFR*. *Oncotarget* 2015;6:5465–74.
25. Hasegawa Y, Ando M, Maemondo M, *et al.* The role of smoking status on the progression-free survival of non–small cell lung cancer patients harboring activating epidermal growth factor receptor (*EGFR*) mutations receiving first-line EGFR tyrosine kinase inhibitor versus platinum doublet chemotherapy: a meta-analysis of prospective randomized trials. *Oncologist* 2015;20:307–15.
26. Kim MH, Kim HR, Cho BC, *et al.* Impact of cigarette smoking on response to epidermal growth factor receptor (EGFR)–tyrosine kinase inhibitors in lung adenocarcinoma with activating *EGFR* mutations. *Lung Cancer* 2014;84:196–202.
27. Kitaguchi Y, Fujimoto K, Kubo K, Honda T. Characteristics of COPD phenotypes classified according to the findings of HRCT. *Respir Med* 2006;100:1742–52.
28. Zhou JY, Zheng J, Yu ZF, *et al.* Comparative analysis of clinicoradiologic characteristics of lung adenocarcinomas with *ALK* rearrangements or *EGFR* mutations. *Eur Radiol* 2015;25:1257–66.
29. Choi CM, Kim MY, Hwang HJ, Lee JB, Kim WS. Advanced adenocarcinoma of the lung: comparison of CT characteristics of patients with anaplastic lymphoma kinase gene rearrangement and those with epidermal growth factor receptor mutation. *Radiology* 2015;275:272–9.
30. Robertson WW, Steliga MA, Siegel ER, Arnaoutakis K. Accuracy of fine needle aspiration and core lung biopsies to predict histology in patients with non–small cell lung cancer. *Med Oncol* 2014;31:967.
31. De Filippo M, Saba L, Concari G, *et al.* Predictive factors of diagnostic accuracy of CT-guided transthoracic fine-needle aspiration for solid noncalcified, subsolid and mixed pulmonary nodules. *Radiol Med* 2013;118:1071–81.
32. Sabri A, Batool M, Xu Z, Bethune D, Abdolell M, Manos D. Predicting *EGFR* mutation status in lung cancer: proposal for a scoring model using imaging and demographic characteristics. *Eur Radiol* 2016;26:4141–7.